

# Extraction of noble metals in a molten salt reactor by helium bubbling

By

Gijs de Boed  
4439104

in partial fulfilment of the requirements for the degree of

**Bachelor of Science**  
in sustainable Molecular Science and Technology

at the Delft University of Technology,  
Faculty of Applied Sciences,  
Dept. of Radiation Science & Technology,  
Reactor Physics and Nuclear Materials,

to be defended publicly on Thursday August 23rd, 2018 at 10.30 AM.

Supervisor:

Dr. Elisa Capelli  
Prof. dr. ir. Jan Leen Kloosterman

Thesis committee:

Dr. Elisa Capelli  
Prof. dr. ir. Jan Leen Kloosterman  
Dr. Anna Smith

## Abstract

The world population keeps growing and along with that the energy consumption. However, the fossil fuels we were used to have plenty of are now depleting. New ways for energy production need to be found. These new ways of energy production need to be environmental friendly, but also efficient. One of the options is nuclear energy.

In this research one nuclear reactor type is emphasized. This type of reactor is the Molten Salt Reactor. This reactor uses a liquid salt fuel which is also used as cooling fluid. The advantages of an MSR are the reduced life time of the fission products and the very safe design. This reactor type is very suitable for the thorium fuel cycle.

Some of the fission products from this thorium fuel cycle need to be extracted from the fuel salt. For example, xenon is formed, which is a neutron poison and needs to be extracted. This is done through an online reprocessing step, called the helium bubbling process. Helium bubbling uses the insolubility of certain fission products in the salt to extract them. It is already used for the extraction of noble gasses from the fuel salt, but it is possible to also use it for the extraction of noble metals.

These noble metals can attach to the surfaces of important reactor components. To prevent this, it is desired to remove the noble metals as well. The goal of this research is to see which parameters influence the helium bubbling process and if these parameters can be optimized to increase the extraction of noble metals from the fuel salt.

The set-up used simulates the bypass of the helium bubbling process in an MSR. It consists of a loop with a venturi tube as bubble generator, a column with a Hallimond tube on top as bubble extractor and a pump to get the liquid flowing through the loop. The used liquid is a mixture of water and glycerol, which have a kinematic viscosity similar to the salt. The particles are molybdenum, as this is one of the real fission products. Finally, the used gas is air, as the density of the gas has very little influence on the process. The bubble size was studied to determine the influence of the liquid and gas flow rate on the bubble size. Also, the efficiency at different gas flow rates was studied to try and find a relationship between this parameter and the efficiency of the process.

The results show that the liquid flow rate has the most influence on the bubble size while the influence of the gas flow rate on the bubble size is not very high. The optimal gas flow rate found in this study is 25 sccm/min.

## Acknowledgements

I would like to thank Dr. Elisa Capelli for all her support with this Thesis project. She was my daily supervisor and was always willing to help me with any problem. Also, I would like to thank Dr. Denis Bykov for helping me choose my thesis project.



# Contents

Abstract .....	2
Acknowledgements .....	2
1 Introduction .....	6
1.1. Molten salt reactor.....	6
1.2. Fission product classification and management.....	7
1.3. Helium bubbling .....	8
1.4. Research goals.....	9
2 Theory .....	10
2.1 Flotation in general .....	10
2.2 Flotation Mechanisms .....	10
2.2.1 Collision frequency .....	10
2.2.2 Stability Efficiency.....	11
2.2.3 Extraction efficiency .....	12
3 Experimental method .....	13
3.1. Selection of particles, fluids and gas.....	13
3.2. Experimental setup.....	13
3.2.1. Bubble generator .....	14
3.2.2. Particle Collector.....	15
3.2.3. Other used equipment .....	16
3.3. Bubble size determination.....	16
3.4. Experimental procedure .....	18
4 Results & Discussion .....	20
4.1. Influence of process parameters on the bubble size.....	20
4.2. Influence of gas flow rate on extraction efficiency.....	21
4.3. Influence of the particle size on extraction efficiency .....	23
4.4. Discussion .....	25
4.4.1 Flow dependency .....	25
4.4.2 Extraction Efficiency .....	25
5 Conclusion and recommendations .....	26
5.1. Conclusion .....	26
5.2. Recommendations .....	26
5.2.1 Further research.....	26
5.2.2 set-up.....	27
References .....	28
Appendix .....	29
A: Results .....	29
A.1: Extracted amounts Mo and efficiencies of the experiments. ....	29
100 mesh .....	29
170 mesh .....	29
3-7 micron .....	29
B: Pictures of other equipment used. ....	30
Pump .....	30
Flowmeter .....	30
C: Macros for picture analysis .....	32
Fixed Liquid flow rate:.....	32
Fixed Gas flow rate: .....	32



# 1 Introduction

## 1.1. Molten salt reactor

Nowadays the world's energy demand keeps on growing and the fossil fuels will not last forever. A lot of research is done to find alternative energy sources and nuclear energy is one of these alternate types of energy. In order to conduct research on nuclear energy as future energy source, an international alliance was forged.<sup>1</sup> This alliance is focussing on six types of reactors, the generation IV reactors, which should be ready for deployment between 2020 and 2030.<sup>1</sup> These reactors are supposed to be on the frontline in sustainability, economics, reliability and safety. This international collaboration is called the Generation IV International Forum (GIF).<sup>1</sup>

One of these Generation IV reactors is the Molten Salt Reactor (MSR). This type of reactor uses a liquid salt as fuel, containing a mix of fluoride salts.<sup>2</sup> One of the ideas of an MSR is to combine the liquid fuel salts with the primary coolant and reprocess it online, but this is not ready for commercialisation yet.<sup>3</sup> The primary coolant is the mixture of lithium and beryllium fluoride and the fuels salts are the uranium and thorium salts. These fuel salts both dissolve easily into the cooling salts and can be easily separated from each other.<sup>1,3</sup> A schematic view of the MSR can be seen in figure 1.1.

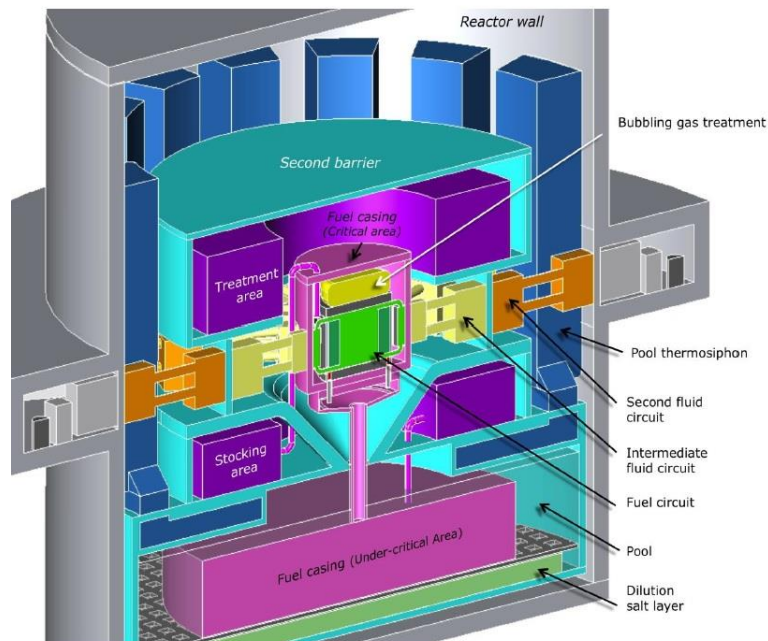
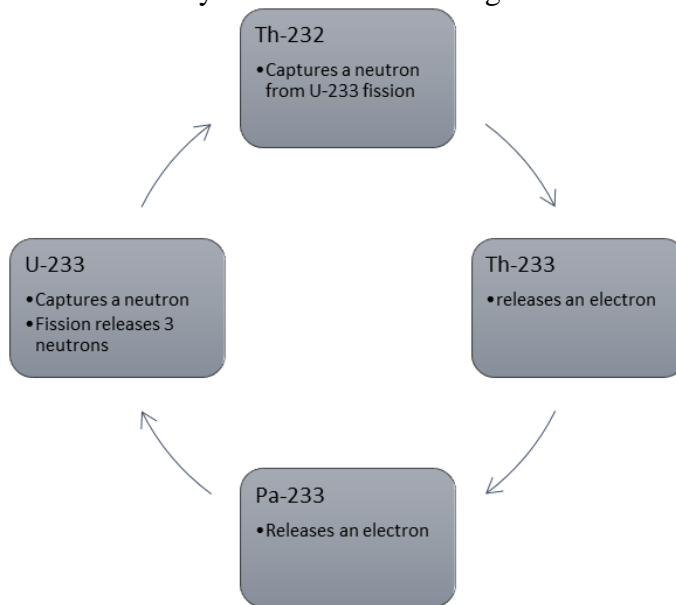


Figure 1.1: cross-section of an MSFR. (Image: daretothink.org)

Before the MSR was implemented in the Generation IV program, the Molten Salt Breeder Reactor (MSBR) concept was developed at Oak Ridge National Laboratory (ORNL). This was a back-up concept for the Fast Breeder Reactor.<sup>3</sup> A reactor prototype, the MSRE operated for four years at Oak Ridge. During this period lots of data were collected on the MSBR and its fuel options. From these data was concluded that there were scale-up problems with the feasibility and the extraction of fission products in the MSR.<sup>3</sup> It was a promising concept and therefore it raised new interests for research when the Generation IV reactors were selected. Since this moment significant changes have been made in the concept to enhance the scale-up possibilities and to enhance the feasibility of the concept.<sup>3</sup>

The MSR is very well suited for the use of the thorium fuel cycle to produce energy<sup>4</sup>. This fuel cycle starts with Th-232, which captures a neutron and this forms Th-233. Th-233 is an unstable isotope that decays into Pa-233 with the release of an electron and finally to U-233. The U-233 also catches a neutron, which causes a fission reaction and hereby releasing 3 neutrons. The neutrons are used to destabilise other Th-232 atoms.<sup>4</sup> A schematic overview of the cycle can be found in figure 1.2.



**Figure 1.2: Thorium fuel cycle. Th-232 captures a neutron and forms Th-233. Th-233 decays to Pa-233 by  $\beta^-$  decay. Pa-233 decays by  $\beta^-$  decay to U-233. U-233 is fissile and absorbs a neutron to start fission. This releases energy and neutrons, which can be captured by Th-232.**

The liquid salt gives the MSR some extra advantages and challenges compared to the normal reactors which work with solid fuels. The burn-up in an MSR is very high. This means that the use of fissile materials is optimized and the ratio fuel to energy is also high. Due to the high burn-up and the online reprocessing, the waste management is very flexible.<sup>4</sup> The production of long-living waste materials is also reduced. The waste that is produced has almost half of the decay time of the waste produced by the other nuclear reactors. Besides advantages in the waste management there are also some advantages on the safety of a reactor. If an accident occurs the fuel salt is automatically drained and stored into cooled storing tanks. This way the fission will stop, and the fuel salt is kept safe.<sup>4</sup>

## 1.2. Fission product classification and management

The fission of uranium results in the formation of a variety of elements. These elements can be divided into three categories based on their behaviour in fluoride salts: noble gasses, noble metals and salt-soluble elements. The first category mostly consists of krypton and xenon.<sup>4</sup> These elements need to be extracted, because some of them are neutron poisons.<sup>4</sup> In this way, the breeding capacity and therefore the performance of the reactor is improved, while also reducing the inventory of fission products.<sup>4</sup>

This gas extraction is done with a so called on-line process. An on-line process means that it takes place in the liquid reactors infrastructure during reactor operation.<sup>4</sup> The process that is used to extract these gasses is called helium bubbling.<sup>5</sup> Helium bubbling, like the name says, is bubbling helium through the fuel salt. The

noble gasses, in this case xenon and krypton, are highly insoluble in the fuel salt and will therefore migrate to any gaseous interface. When helium is bubbled, a gaseous interface will be available at the bubbles. This is the main reason that helium bubbling is a very effective way to extract the xenon and krypton from the fuel salt.<sup>4</sup>

The second group are the noble metals. These will deposit on the surfaces of heat exchangers and pumps etc.<sup>4</sup> This could create some complications, because the heat exchangers might stop cooling, which means the temperature will rise, which could create a meltdown at the reactor. This is not the only reason that makes the extraction interesting. There is also molybdenum formed in the fission reaction of U-233, which is highly used for medical applications.<sup>4</sup>

It is found that a small amount of these noble metals also attaches to the bubbles from the helium bubbling process. This makes it even more interesting. The process that makes this happen is flotation. This is a process where particles attach to bubbles and are taken to the surface of the liquid, where the particles can be collected.<sup>6</sup> In the flotation process the metal particles will attach to the helium bubbles, which transports the particles to the surface. When the particles reach the surface, they can be captured and treated.<sup>6</sup>

### 1.3. Helium bubbling

As mentioned before, much research was conducted into the MSR at Oak Ridge National Laboratory. One of these researches was conducted on the helium bubbling in the reactor. At the time, not much literature could be found on how to implement a bubbling system into a reactor.<sup>7</sup> Therefore, they started experimenting and concluded that a venturi device worked best as a bubble generator in the MSBR. The gas was injected into the venturi throat and the bubbles were generated by the turbulence of the fluid.<sup>7</sup>

Once the bubbles were in the fuel and were enriched in fission gas, they had to be separated from the fuel. To do so they chose to use a pipeline bubble separator. This separator was chosen because of its high performance and low volume inventory.<sup>7</sup> At ORNL they also had experience with this kind of separator, because they had already used it before in a research called the Homogeneous reactor Test. The pipeline bubble separator uses swirl vanes to create an artificial gravity field, which causes the bubbles to migrate to the gaseous core of the separator.<sup>7</sup>

Both the generator and the separator were designed to be installed in a bypass stream around the fuel pump, as can be seen in figure 1.3



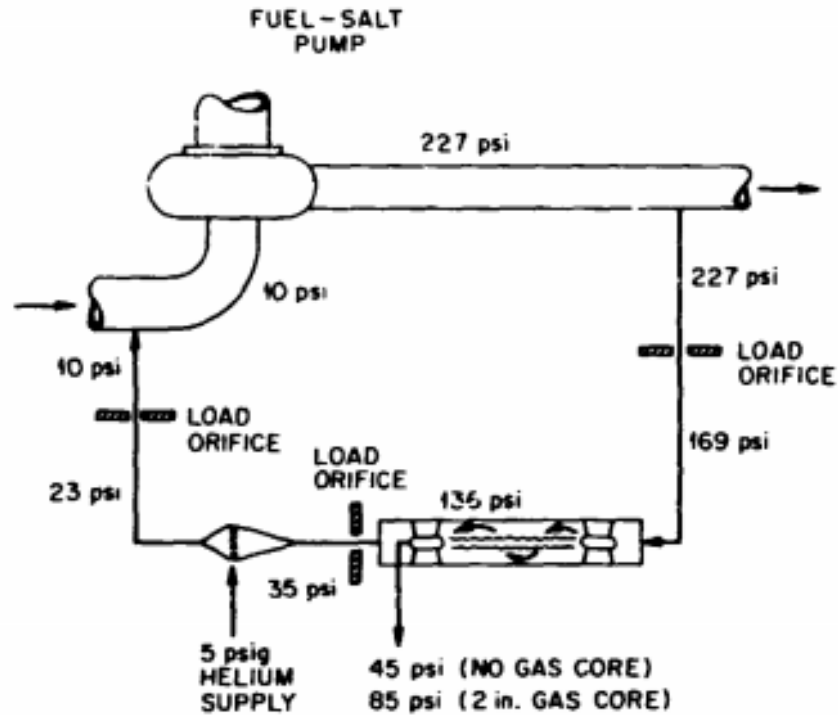


Figure 1.3: Schematic view of the bubble generator and removal bypass.<sup>7</sup>

#### 1.4. Research goals

The efficiency of the helium bubbling process depends on various variables. The two most important and controllable variables are the bubble size and the liquid flow rate.<sup>6</sup> The particles can only attach to bubbles that are large and stable enough to hold them. The liquid flow rate also effects the bubble size. If the volume rate gets higher the bubbles get smaller, because with increasing rate the turbulence of the flow also increases. This makes the bubbles more unstable and then they may explode or split into smaller bubbles.<sup>6</sup> The goal of this research is to determine the influence of some of the variables of the helium bubbling process and how these variables can be optimised to enhance the extraction of noble metals from a MSR.<sup>6</sup>

# 2 Theory

## 2.1 Flotation in general

Flotation is a separatory method to separate particles from a liquid slurry<sup>8</sup>. Currently the main application of froth flotation is in the mineral industry and waste-water treatment.<sup>6</sup> Its main use in the mining industry is to gain clean concentrates of a mineral or metal from the ores. The ores are crumbled and mixed with water and reagents.<sup>9</sup> Then air is passed through to which the metal/mineral particles will attach. The particles float to the surface where they can be collected.<sup>10</sup> In waste-water treatment, the flotation process is applied to extract harmful or poisonous surfactants from the water.<sup>8</sup>

Besides these there are many other applications of flotation in the nowadays industries.<sup>11</sup> Some applications are given in table 2.1.

Species recovered	Recovered from	Industrial process or interest
Non-ferrous metal sulfides (Cu, Pb, Zn, Ni, Co, Mo, Hg, Sb)	Mineral ores	Metal production
Potassium chloride	Potash	Fertilizer
Coal fines	Ash-producing shales and rocks, and SO <sub>2</sub> emission-producing metal sulfides	Electric power
Ink particles	Waste paper	Paper recycling
Silver	Photographic materials	Recycling
Copper	Acid mine effluents	Metal production
Bitumen	Oil sands	Petroleum industry

**Table 2.1: Main applications of the flotation process. The recovered species and what the material from which it is recovered is given.<sup>12</sup>**

## 2.2 Flotation Mechanisms

### 2.2.1 Collision frequency

In equation 2.1 the change in particle concentration is given as a function of the overall collection efficiency of the bubble  $E_{coll}$  or as a function of the efficiencies of the subprocesses from the bubble-particle collisions; collision  $E_c$ , attachment  $E_a$  and stability  $E_s$ . By taking the product of these efficiencies and the collision frequency, the change of particles can be determined for a stirred vessel reactor.<sup>6</sup>

$$\frac{dN_p}{dt} = -kN_p = -Z_{pb}E_{coll} = -Z_{pb}E_cE_aE_s$$

**Equation 2.1: Change in number of particles as a function of efficiencies and collision frequency.<sup>6</sup>**

An important aspect of the flotation process is the collision between bubbles and particles. When these two collide a bubble particle aggregate is formed which floats to the surface of the floatation cell.

$$Z_{pb} = 5N_pN_b\left(\frac{d_b}{2}\right)^2\left[\frac{0.33\varepsilon^{4/9}d_b^{7/9}}{\nu^{1/3}}\left(\frac{\Delta\rho}{\rho}\right)^{2/3}\right]$$

**Equation 2.2: Collision frequency between bubbles and particles per unit volume<sup>6</sup>**

Equation 2.2 shows that the collision frequency  $Z_{pb}$  depends mostly on the amount of bubbles and particles, but also on the bubble diameter. The other parameters in equation 2.2 are; the difference in density between the particle and the liquid  $\Delta\rho$ , the energy dissipation rate  $\varepsilon$  and the kinematic viscosity  $\nu$ .<sup>6</sup>

### 2.2.2 Stability Efficiency

Besides the collision rate, the stability is also an important factor in the flotation process. When an aggregate is formed it is important that it remains until it has reached the surface of the flotation cell. The stability of the aggregate can be determined with the use of equation 2.3.

$$E_s = 1 - \exp \left\{ 1 - \left( \frac{d_{p\max}}{d_p} \right)^2 \right\}$$

**Equation 2.3: Bubble-particle aggregate stability efficiency in a turbulent field.**<sup>6</sup>

It can be seen in equation 2.3 that the stability of the aggregate depends on the size of the particles and the maximum particle size. The maximum particle size ( $d_{p\max}$ ) depends on the value of  $b_m$ , as can be seen in equation 2.4.

$$d_{p\max} = \left( \frac{3\gamma(1 - \cos \theta)}{\Delta\rho(g + b_m)} \right)^{1/2}$$

**Equation 2.4: Maximum particle diameter in a turbulent field.**<sup>6</sup>

The maximum particle size also depends on the contact angle  $\theta$  and the surface tension  $\gamma$ .

This parameter  $b_m$  is the centrifugal force on the particle because of the attachment of the particle to a bubble. The value of  $b_m$  can be determined with equation 2.5.

$$b_{m(d_{b\max})} = \frac{1.9\varepsilon_i^{2/3}}{d_{b\max}^{1/3}}$$

**Equation 2.5: Centrifugal force as a function of the energy dissipation and the maximum stable bubble size.**<sup>6</sup>

The final equation needed to be able to derive the stability of the bubble-particle aggregate is the equation for the maximum stable bubble size. This equation can be found in equation 2.6.

$$d_{b\max} = 3.27 \left( \frac{\gamma^{3/5}}{\varepsilon^{2/5} \rho_L^{3/5}} \right)$$

**Equation 2.6: Maximum stable bubble diameter in a turbulent field.**<sup>6</sup>

By substituting equation 2.4, 2.5, and 2.6 in equation 2.3 an expression can be found for the stability efficiency for the bubble-particle aggregate. This leads to equation 2.7.

$$E_s = 1 - \exp \left\{ 1 - \frac{1.17\gamma^{6/5} \sin \theta_R \sin \Delta\theta}{d_p^2 \Delta\rho \varepsilon_i^{4/5} \rho_L^{1/5}} \right\}$$

**Equation 2.7: Bubble-particle aggregate stability efficiency in a turbulent field.**<sup>6</sup>

The expression for the maximum bubble size is simplified, but the function for the normal bubble size is rather complicated and therefore research is needed to determine this.

### 2.2.3 Extraction efficiency

Now that the stability of the aggregates can be determined, we can try to determine the collection efficiency of the aggregates. The equation for the diffusive collection efficiency can be calculated with equation 2.8.

$$E = \frac{4k_p(c - c_s)}{cU} = 4f(Sh/Pe) = f(Pe)^{-2/3}$$

$$Sh = \frac{2r_b k_p}{D}$$

$$D = \frac{k_B T}{6\pi\mu r_p}$$

#### Equation 2.8: Diffusive collection efficiency with the Sherwood number and the diffusivity<sup>6</sup>

When the collection efficiency needs to be determined, the diffusivity and the Sherwood number are to be determined. A recurring parameter in these equations is the particle radius. When this cannot be determined the concentration of the particles in the bulk ( $c$ ) and in the bubble surface ( $c_s$ ) can be used.

From equations 2.1 to 2.8 it is seen that there are some important parameters for the flotation process. Some recurring parameters are the bubble and particle size and the density of the liquid. Also, the turbulence in the flotation cell is of importance, because these equations are all based on a turbulent liquid flow.

# 3 Experimental method

## 3.1. Selection of particles, fluids and gas

Simulant fluids and gas are used in the present setup, with the advantage of simplifying material requirements and procedure. This is, because a molten salt requires a very high operation temperature and is also very corrosive. To simulate the conditions of the helium bubbling system in a MSR, a liquid, a gas and the particles had to be chosen. The liquid had to be chosen in such a way that it would follow the same dynamics of the fuel salt. A mixture of water and glycerol was chosen, which has the same kinematic viscosity as the fuel salt. In fact, the dynamics of a fluid are dependent on the Reynolds number ( $Re$ ), and on itself  $Re$  is dependent on the kinematic viscosity:

$$Re = \frac{uL}{\nu}$$

**Equation 3.1:** Equation to calculate the Reynolds number.

where  $u$  is the velocity of the fluid with respect to the object (m/s),  $\nu$  is the kinematic viscosity ( $m^2/s$ ) and  $L$  is a characteristic.

In table 3.1 the comparison between the properties of the molten salt and the water glycerol mixture can be found.

Property	Molten Salt (LiF-BeF <sub>2</sub> -ThF <sub>4</sub> )	Water/glycerol
Content	70.06-17.96-11.98 mole %	64/36 vol%
Density (kg/m <sup>3</sup> )	2.69E3	1.104E3
Dynamic viscosity (Ns/m <sup>2</sup> )	1.032E-3	4.234E-3
Kinematic viscosity (m <sup>2</sup> /s)	3.836E-6	3.834E-6

**Table 3.1:** Properties of the molten salt and the simulant water/glycerol mixture.<sup>13</sup>

The chosen gas was air, because the density of the gas has very little influence on the efficiency and bubble-particle aggregation. For these calculations the difference in density between the gas and the liquid is taken but since the density of the gas is almost  $10^3$  times smaller than the density of the liquid, the difference is negligible. Therefore, the cheapest option was taken which is air.

For the particles molybdenum was chosen. An isotope of molybdenum is one of the fission products in an MSR and therefore molybdenum particles are very well suited to simulate the extraction of the particles with.

## 3.2. Experimental setup

For the setup to meet up with the reality a loop was built to simulate the liquid flow in an MSR. The largest part of the loop is made of polyvinylchloride pipes, except for one part where there is a Plexiglass tube. This was done to make it possible to take photos of the bubbles and the bubble-particle aggregates. In the pictures below there is a computer made overview of the loop (fig 3.1). The equipment will be described in more details in the next section.

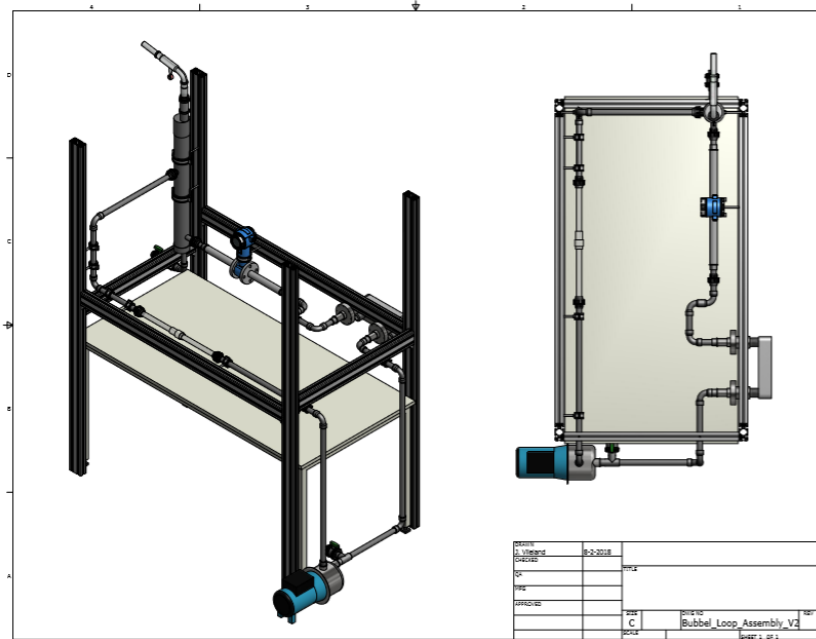


Figure 3.1: Digital made overview of the bubble loop

### 3.2.1. Bubble generator

#### Venturi tube

The Venturi tube is used to accelerate the liquid flow and increase the uptake of the air from the inlet. The tube is smaller in the middle and because the flow rate is kept constant the velocity of the fluid will increase at the constricted area of the tube. Because of this increase in velocity, the pressure will drop behind the constricted part. This is due to Bernoulli's law for the conservation of mechanical energy<sup>14</sup>. Around this constricted area a little ring was placed with small inlets into the tube. This is where the gas enters the tube and the bubbles are created.

The used venturi tube was special made so that it could also be used as a gas distributor for the inlet of air into the loop. It ensures the formation of very small and uniform bubbles and also has the advantage of being compatible with a molten salt operation.

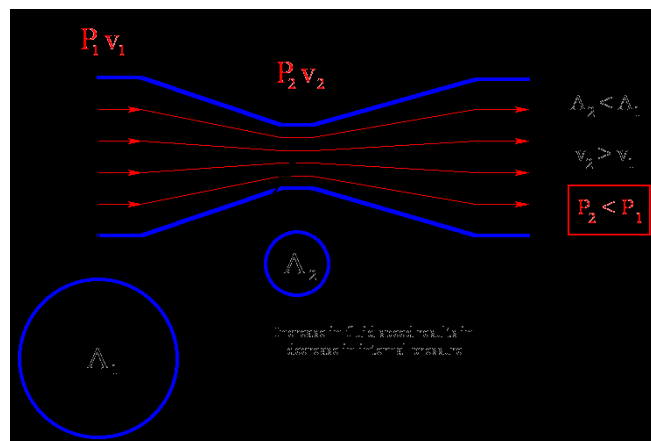


Figure 3.2: Schematic drawing of the Venturi tube.<sup>14</sup>

## Gas flow

The gas introduced in the system is compressed air. To control the gas flow into the loop a Bronkhorst gas flow controller was used. This controller is linked to a computer on which it can be directed with two softwares: FlowDDE and FlowView. FlowDDE links the computer to the gas controller and establish that the connection is solid. With FlowView the amount of gas can be set to the desired value. Between the controller and the compressed air outlet, a pressure controller was set. This is to reduce the pressure of the compressed air to a desired value. A meter on the pressure controller shows the outlet pressure.

From the controller, the air goes to the venturi tube, where it first enters a little gas compartment and when the pressure is high enough the air enters the tube through the holes in the venturi tube. The air is introduced all around the tube as the holes are radially distributed. This was done to enhance an even bubble distribution.

To introduce the bubbles into the loop, little holes (0.8 mm) were made in the small part of the venturi tube, as can be seen in figure 3.3.

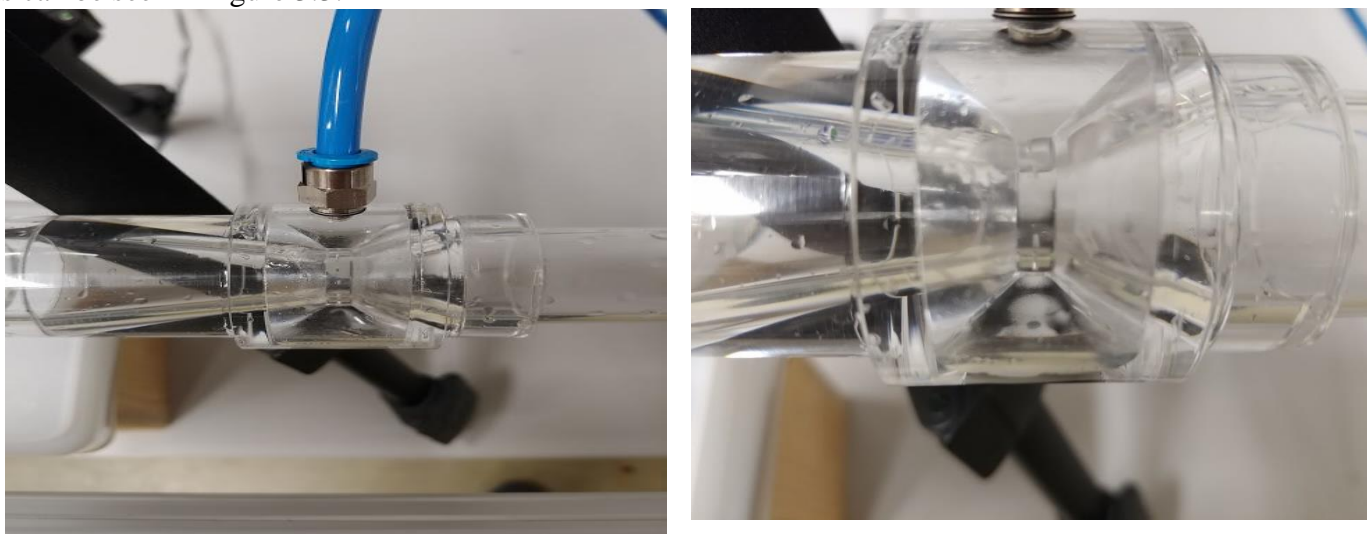


Figure 3.3: Venturi tube with the small gas compartment around it. Holes are made in the contracted part of the tube to introduce the gas through

### 3.2.2. Particle Collector

To collect the bubbles on the top of the column, a Hallimond tube was used. The bend in the Hallimond tube is very well suited to collect the particles. The bend is made in such a way that the particles will not detach from the bubbles when they collide with the tube wall. Next to the connection of the Hallimond tube and the column there is a small reservoir in which the particles are collected that sink down from the liquid-gas interface. Underneath this small reservoir there is a valve, which allows for opening and closing of the reservoir to take samples. In figure 3.4 the used Hallimond tube is shown.



Figure 3.4: The used Hallimond tube to capture the particles with and the bend tube that was placed on top of the Hallimond tube to enlarge its capacity.

### 3.2.3. Other used equipment

- A Nastec Mida pump was used to introduce a flow into the loop. (Appendix B)
- Flow meter (appendix B)
- A jerrycan to store the mixture in.
- FlowDDE and FlowView software (Appendix B)
- Small tubes to store the samples in.
- An oven to warm the samples to 110 °C
- An oven to burn the filtration paper at 510 °C
- A balance to weigh the particles
- Ceramic cups to burn the particles in.
- Heat exchanger

### 3.3. Bubble size determination

To determine the influence of the different flow rates on the bubble size pictures of the bubbles in the loop were taken. The pictures were taken with a Nikon 1 J5 camera with a Nikon DX Af-S Micro Nikkor 40mm 1:2.8G lens mounted (figure 3.5). Also, a light was put underneath the tube to make the bubbles more visible.

First a fixed gas flow was taken, and the liquid flow was changed. Second the liquid flow was fixed, and the gas flow was variable. This was done to get a clear idea on the influence of each flow rate individually on the bubble size. The pictures were taken just after the Venturi-tube with the gas inlet. This is done to see what the size of the formed bubbles is before it goes into the flotation process.



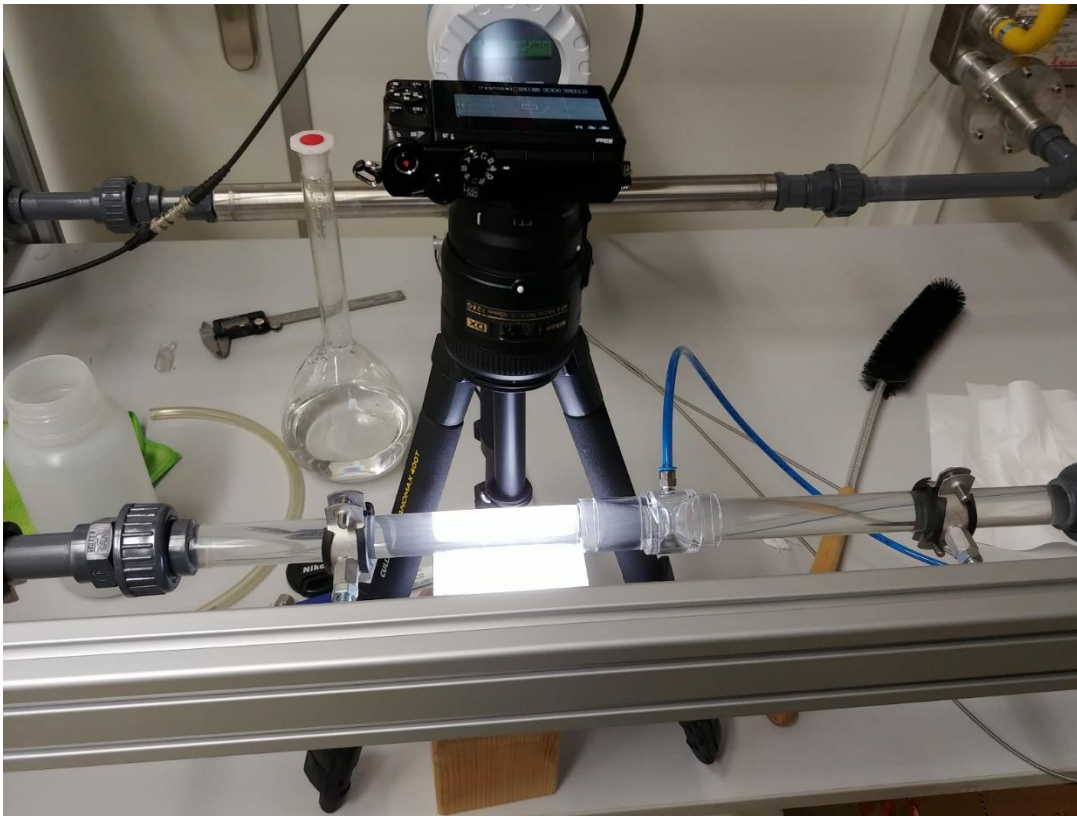


**Figure 3.5: Set-up for taking pictures and videos of the bubbles.**



**Figure 3.6: Picture of the bubbles generated in the loop. Liquid flow = 044 l/s and gas flow = 10 cm<sup>3</sup>/min**

The pictures were treated using image analysis with ImageJ software. This program allows the user to automatically process pictures and analyse them for different subjects.

First the scale of the picture was determined by using the width of the tube. This is 24.86 mm and therefore an easy standard to set the scale. Then the picture is cropped to get a clearer view of the bubbles. The cropped image is converted into an 8-bit image to facilitate the change of the threshold of the picture. When the threshold has been optimized to get the bubbles highlighted, the picture is made binary. This removes most of the background noise (figure 3.7).



Figure 3.7: Bubbles inside the loop after processing picture. Liquid flow = 037L/s and gas flow = 5cm<sup>3</sup>/min

The program is now able to analyse the amount and size of the particles in the picture. The settings can be changed so the program will take ellipses as particles. This gave a list of results which also included the areas of the bubbles. From these areas a mean was calculated by the program and from this the mean bubble diameter could be determined. These results can be seen in the next chapter.

The macros that are used to automatize the analysis of the bubbles can be found in Appendix C.

### 3.4. Experimental procedure

The efficiency of the helium bubbling process can be determined by introducing a known number of particles into the loop and measuring the amount that has been extracted after the process has been running for 80 minutes. After that the extracted amount becomes almost constant. Molybdenum particles of different sizes were used, as these are one of the particles that are expected to be extracted in the MSR.

#### Sampling

First, the water-glycerol mixture needs to be filtered before each experiment. The mixture has a glycerol volume percentage of ~31%, determined by calculating the kinematic viscosity of the molten salt mixture.<sup>4</sup> The loop is filled with the mixture and then it is run at the lowest liquid flow rate to pump the air out. In the meantime, a known amount of particles are weighted and prepared to be added.

When the loop is ready the settings are entered and then the particles can be added. Samples are taken at 10, 20, 40 and 80 minutes to get a curve for the yield. For the final sample, the tube is drained completely. In this way, the particles that have deposited on the wall can be extracted.

#### Filtration

For the filtration of the samples and for the filtration of the mixture the same sort of set-up was used, only at a different size. A small 500 ml Erlenmeyer flask was used to capture the filtrate in for the different samples. Special filters were used which leave no ashes when burnt. These were chosen to enable an accurate weighing of the extracted particles after burning the filters. With this the yield could be determined. These filters were folded in half two times to make them fit for the filtration funnel. This funnel was placed in a rubber stopper. This was placed on top of the Erlenmeyer which was then placed under vacuum to accelerate the filtration process.

For the filtration of the mixture a 2L Erlenmeyer was used to hold the filtered mixture. Also, a 4L beaker was used to store the mixture in. On top of the Erlenmeyer a rubber ring was placed to narrow the top. A sieve with pores was then placed at the top and covered with a filter. Normal filters were used, differently from the previous filtration set-up. After filtration the mixture is once again stored in a cleaned jerrycan.

After the samples are filtered, they are put in a drying oven which warms up to 110 °C. This is done to dry the filters. The samples are kept in the heater for about 20 minutes. After this the filters are put in ceramic crucibles. These crucibles are put in an oven and are heated up to 510 °C to burn the filters. The filters that are used are ash-free filters, so that the mass of the collected particles can easily be weighed. In the oven molybdenum oxide is formed. Therefore, the weight of the particles that are left have to be corrected. It was found that the oxide that is formed is MoO<sub>3</sub>. The percentage of molybdenum in this compound is about 66.65%. This is also the factor for which the weighed particles need to be corrected. The results from this correction can be used to determine the efficiency of the bubbling process.

This procedure is followed for different gas flow rates. The gas flow rates were chosen after the first run of the loop with 100 mesh particles. The flow rates are 5, 15, 25, 35 and 45 cm<sup>3</sup>/min.

# 4 Results & Discussion

## 4.1. Influence of process parameters on the bubble size

Pictures were taken at different fixed flow rates for both gas and liquid flows.

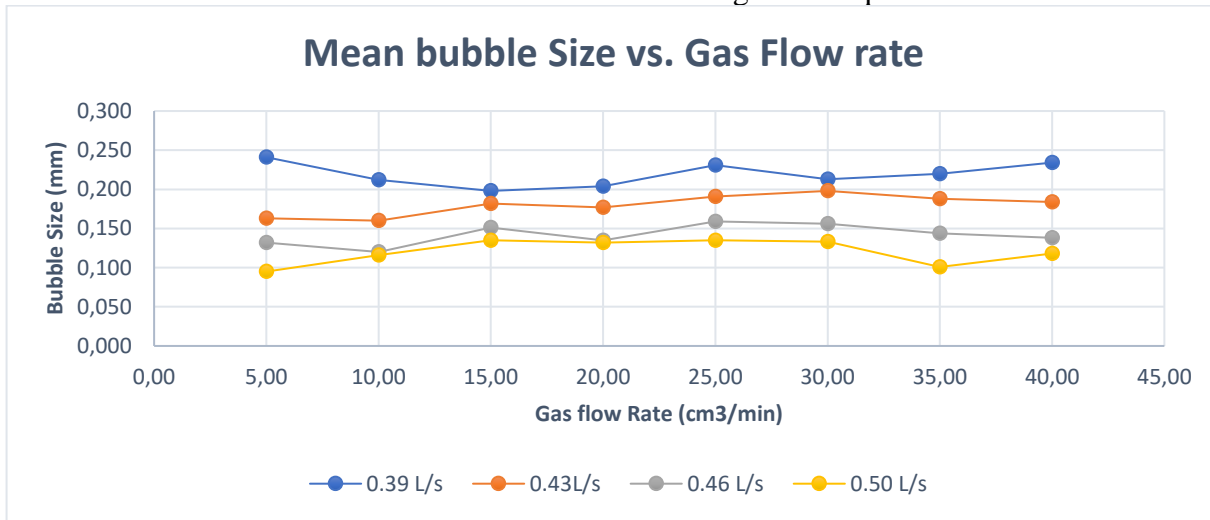


Figure 4.1: Mean bubble diameter as a function of the inlet volumetric gas flow rate for a fixed liquid flow rate.

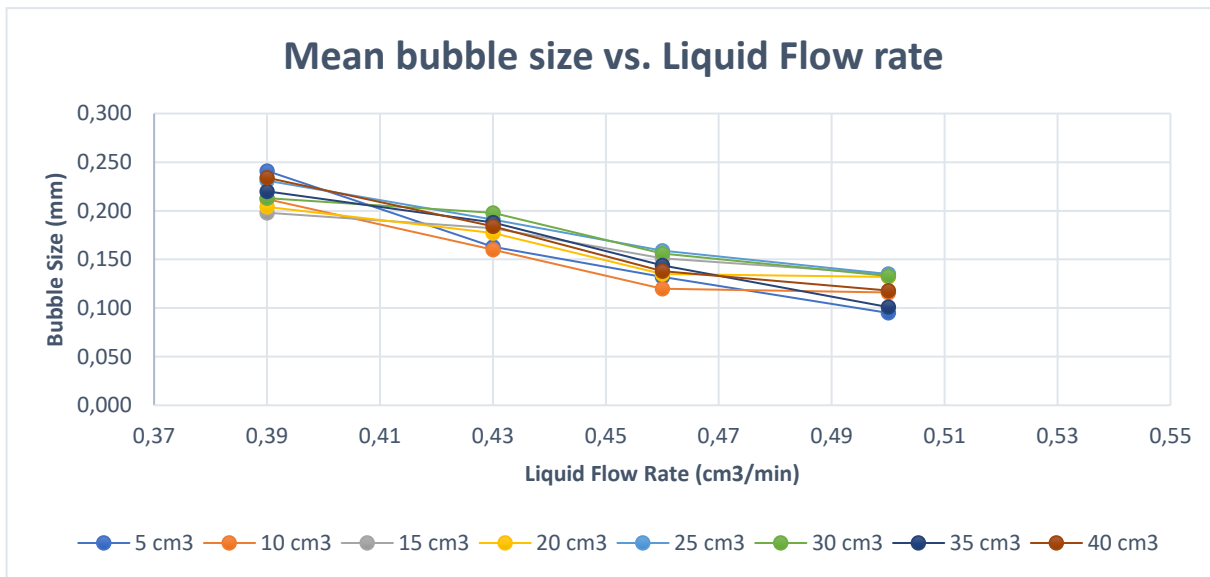


Figure 4.2: Mean bubble diameter as a function of the liquid flow rate for a constant gas flow.

Figure 4.1 and 4.2 show the behaviour of the mean bubble size as function of different parameters. In figure 4.1 the lines are quite stable with no large fluctuation. Also, it is clear that the bubble size is smaller for higher liquid flow rates. This is more clear in figure 4.2 where the influence of the liquid flow rate is reported. The exact values of the mean bubble sizes can be found in table 4.1

Gas Flow rate (cm <sup>3</sup> /min)	0.39 L/s (mm)	0.43 L/s (mm)	0.46 L/s (mm)	0.50L/s (mm)
5.0	0.241	0.163	0.132	0.095
10.0	0.212	0.160	0.120	0.116
15.0	0.198	0.182	0.151	0.135
20.0	0.204	0.177	0.135	0.132
25.0	0.231	0.191	0.159	0.135
30.0	0.213	0.198	0.156	0.133
35.0	0.220	0.188	0.144	0.101
40.0	0.234	0.184	0.138	0.118

**Table 4.1: Table with the mean bubble sizes at fixed flow rates and different gas flow rates**

## 4.2. Influence of gas flow rate on extraction efficiency

The experiments were performed with three different particle sizes. The arrangement of set-up for these experiments is the same as used for the bubble size determination. The only difference is that particles are dissolved in the mixture with a concentration of approximately 0.212 g/L<sup>15</sup>. This concentration was determined to be the concentration of the particles in the MSR and therefore used in the experiments.

In figure 4.3, 4.4 and 4.5 the extracted amount of molybdenum is shown as a function of time. As noticed before the experiments were done at different gas flow rates. The lines indicate the increase in yield over time and the separate dots indicate the total yield after collecting the particles from the inside of the Hallimond tube as well. Particles precipitated on the inside of the tube which means they are collected, but not captured in the samples.

The exact values of the extracted Mo can be found in appendix A.2

### 100 mesh

These particles have a size of approximately 0.15 mm in diameter.

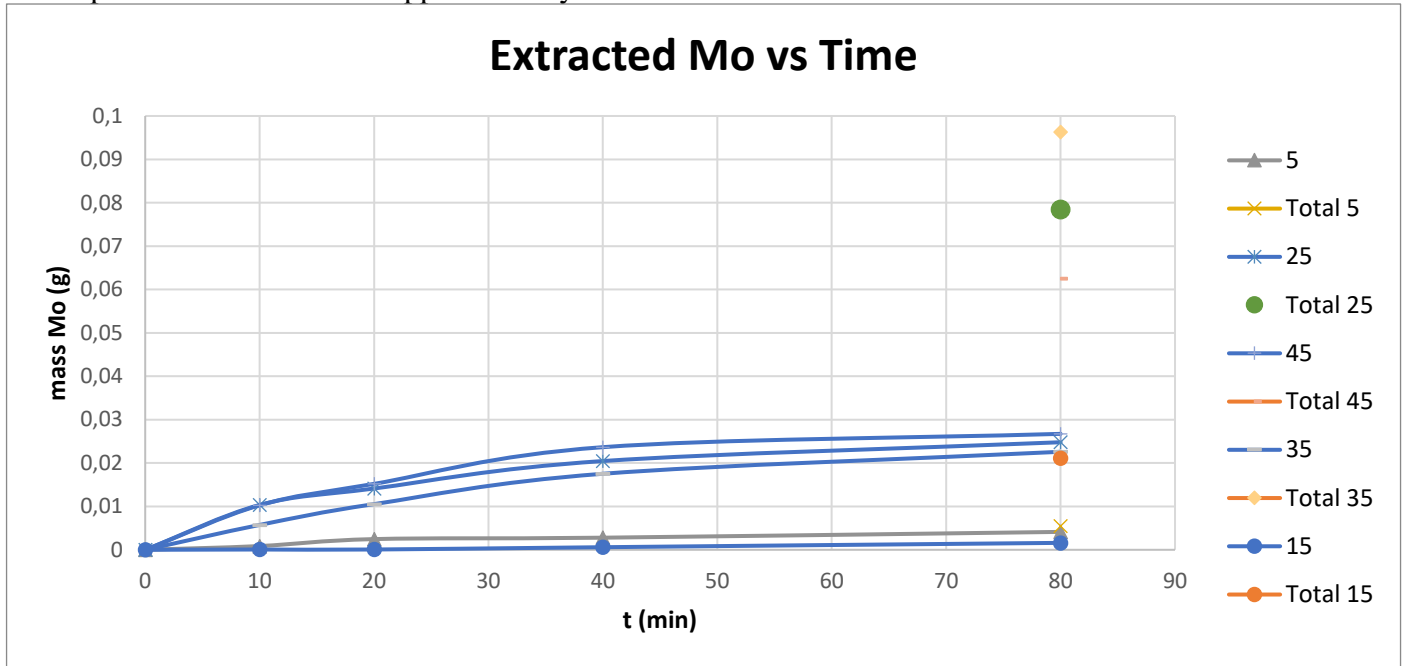


Figure 4.3: The extracted amount of Mo plotted against time. The amounts are given for different gas flows.

### 170 mesh

These are particles with an average size of 88 micrometer.

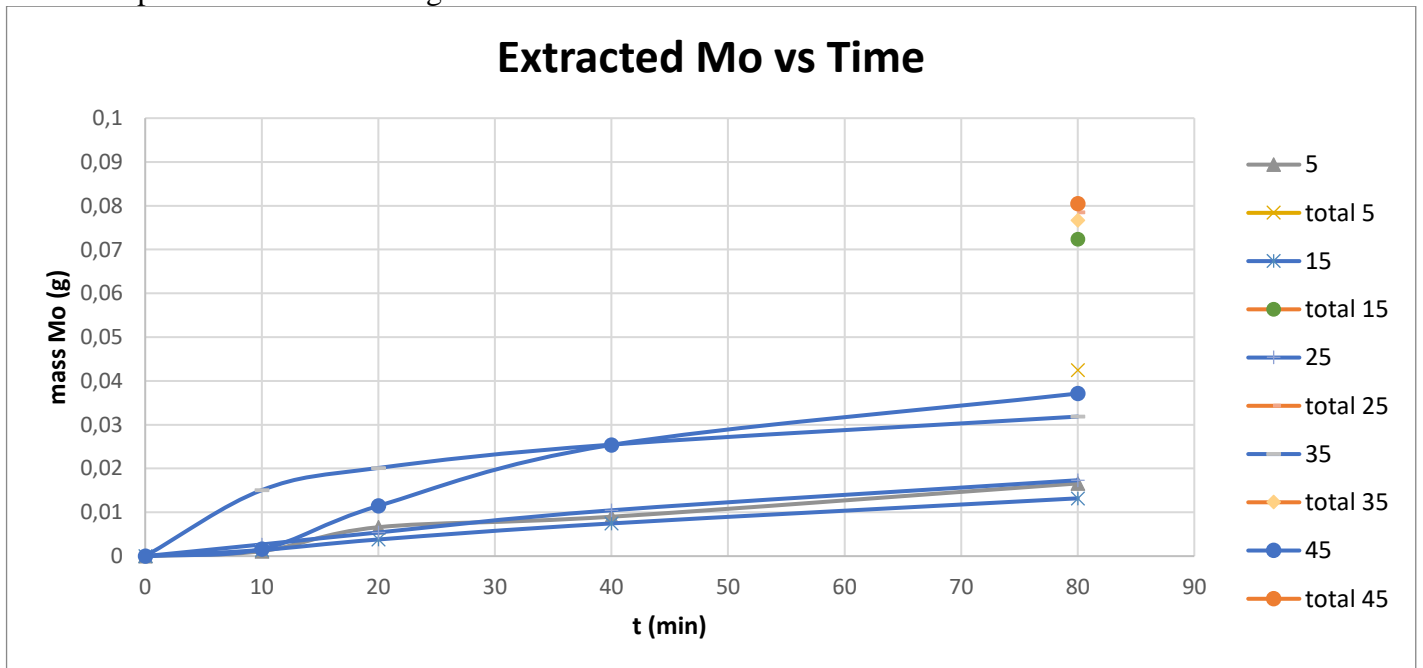


Figure 4.4: The extracted amount of Mo plotted against time. The amounts are given for different gas flows.

3-7 microns

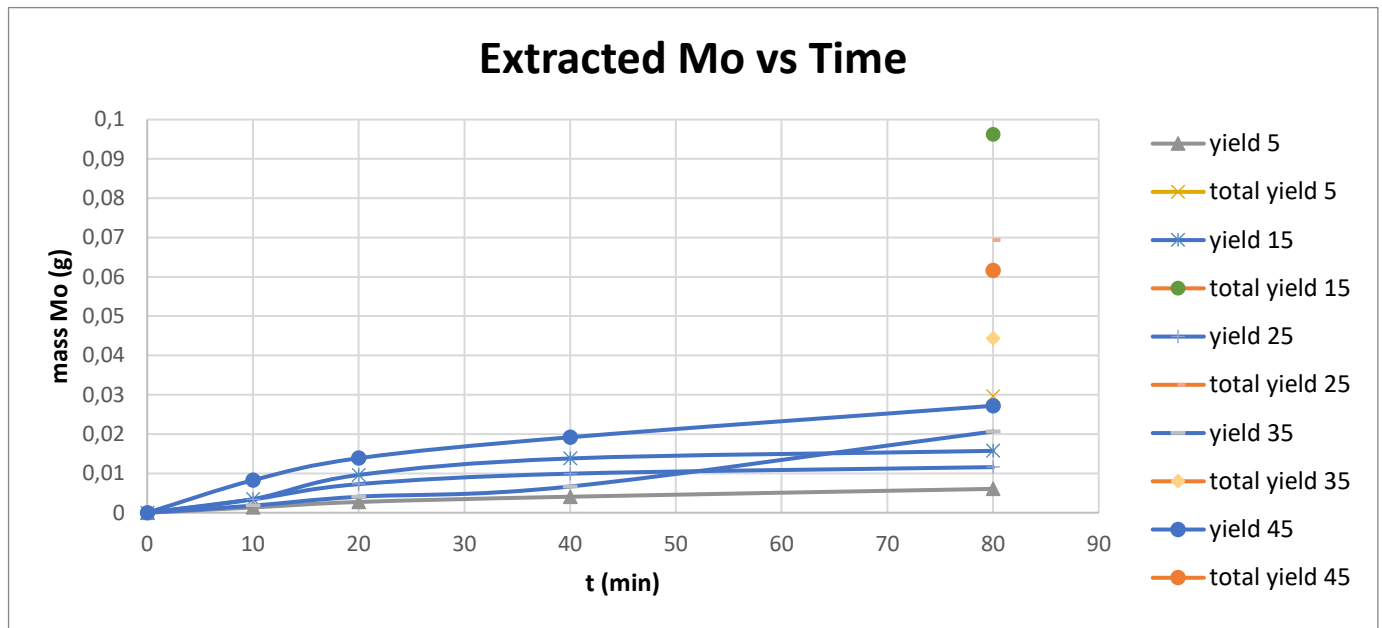


Figure 4.5: The extracted amount of Mo plotted against time. The amounts are given for different gas flows.

### 4.3. Influence of the particle size on extraction efficiency

Figure 4.6, 4.7 and 4.8 show the efficiency of the extraction process. The efficiency is based on the total extracted amount of molybdenum. This means it includes the amount that precipitated on the inside of the tube. All the efficiencies were determined at the same liquid flow rate of 0.41 l/s.

100 mesh

These particles have a size of approximately 0.15 mm in diameter.

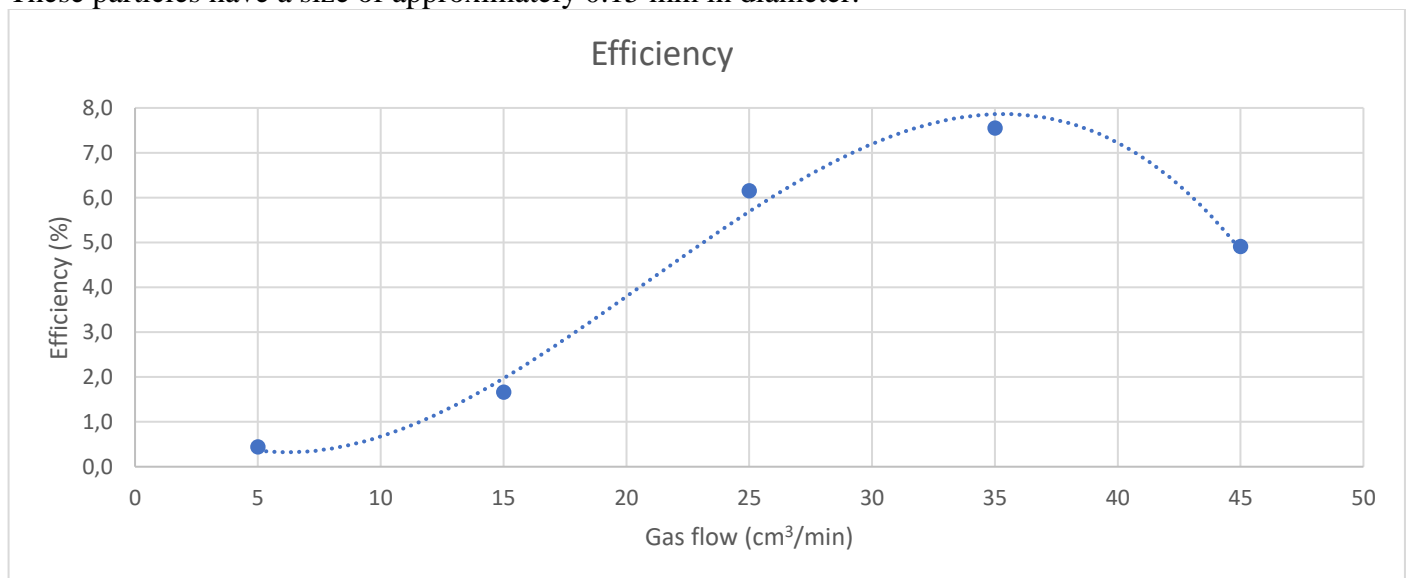


Figure 4.6: Efficiency of the bubbling process given for different gas flows.

**170 mesh**

These are particles with an average size of 88 micrometer.

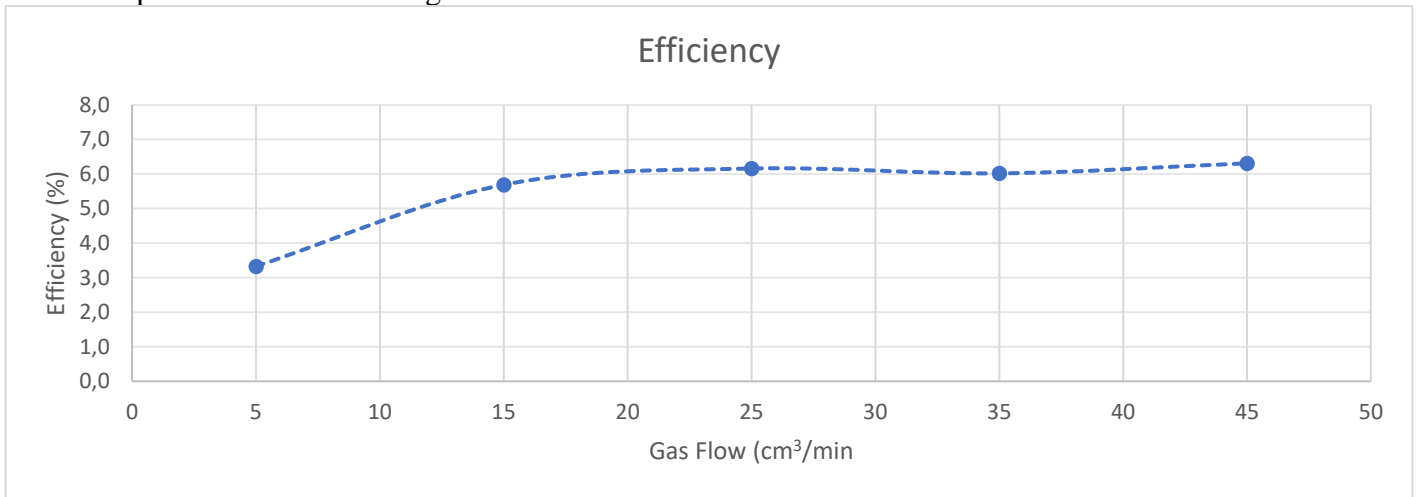


Figure 4.7: Efficiency of the bubbling process given for different gas flows.

**3-7 microns**

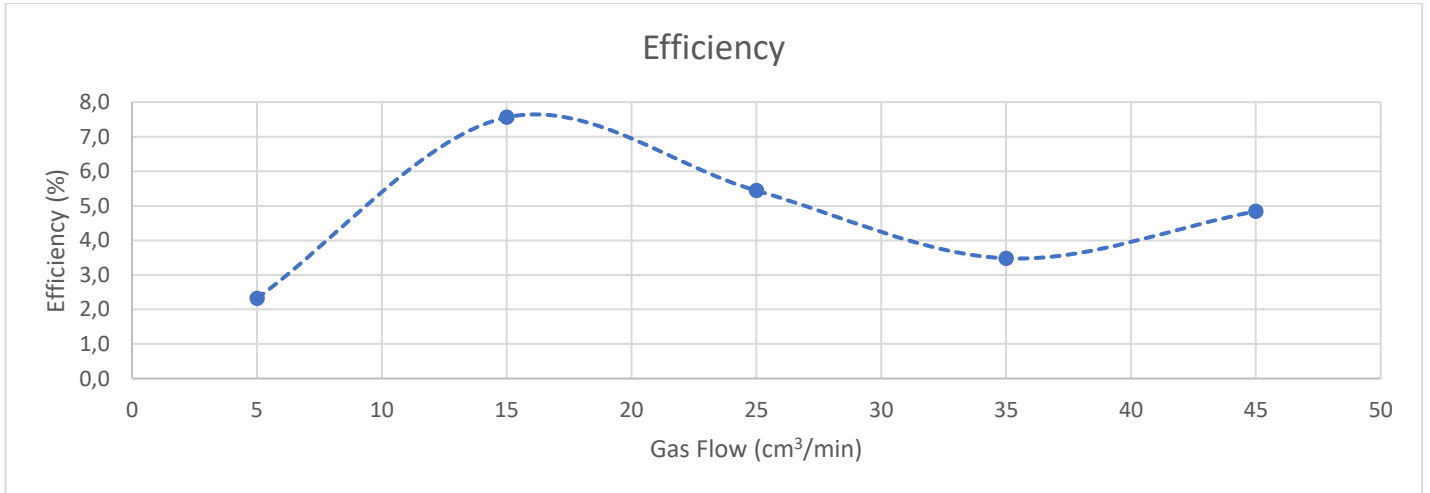


Figure 4.8: Efficiency of the bubbling process given for different gas flows.



## 4.4. Discussion

### 4.4.1 Flow dependency

The results from this part of the study are in the line with the expectations. As the gas inlet can only let a certain amount of air into the tube, the gas flow was expected to have little effect on the bubble size. In addition to the physical phenomenon, the fluctuation that is seen in the graphs can be caused by the uncertainties in analysing the pictures. Two sources of uncertainty have been observed. In the first case, the program recognizes ellipses in the noise in the background. This can be causing a decrease in the mean bubble size. The second effect is due to the overlapping of bubbles in the pictures which gives a raise in the mean bubble diameter in some points. The program then sees this as one ellipse and this causes an increase in the mean bubble size. The results clearly showed that the bubble size for an increasing gas flow rate is almost constant while the bubble size for an increasing liquid flow rate is clearly decreasing.

### 4.4.2 Extraction Efficiency

In figure 4.3 all the curves for the extraction efficiency of the 3-7 micrometer particles follow the same trend for the yield. This is in line with the expectations, as the yield is expected to increase fast in the beginning and then stabilize after some time. This is due to the decrease in particle concentration which results in less collisions of bubbles with particles.

The yield for 5 and 15 cm<sup>3</sup>/min is very low. These lines also follow the same trend but are much smaller than the other yields. This could be due to the fewer bubbles that are generated, because the gas flow is lower. Therefore, the larger particles cannot effectively attach to the bubbles. In figure 4.6 this is also seen in the efficiency of the process. This efficiency is very low for low gas flows but increases when the gas flow increases too. The efficiency is highest at 35 cm<sup>3</sup>/min. At higher gas flows the efficiency decreases. This can be due to the increase in turbulence because of the increasing bubble density. If the flow gets more turbulent the particles will detach from the bubbles much easier.

Figure 4.4 shows the same behaviour for particles of 88 micron. The difference between the two is that in this figure the yield increases with the flow rates. This is also clearly visible in figure 4.7. Here it is shown that the efficiency of the process increases somewhat faster with the first step but then slightly keeps increasing. This means that this size of bubbles and bubble density is working very well for this size of particles. The particles have a steady attractive and repulsive interactions, which results in this type of efficiency curve.

In figure 4.5 behaviour of the curves is the same as the 170 mesh particles. Only the total extracted mass is more for the 25 cm<sup>3</sup>/min. In this case, as shown in figure 4.8 the efficiency curve has more the shape of the curve from figure 4.6 it starts with a fast increase, then reaches an optimum and starts declining. Due to the small size of these particles it is logical that they also attach well at low gas flows. At the higher flow rates, the particles will detach easier due to the increase of turbulence in the flow.

The efficiency at higher flow rates might be lower than the real value due to foam production. At high flow rates more foam is produced at the liquid-gas interface and can result in a number of particles extracted but not collected in the sample.

In an MSR system. the 3-7-micron particles are the most realistic, because that is also approximately the size of the particles. The other particle sizes are used to determine if a relationship between the particle size and the efficiency could be found.

# 5 Conclusion and recommendations

## 5.1. Conclusion

From the results that were obtained on the determination of the average bubble in water-glycerol solution it can be concluded that the liquid flow rate has more influence on the bubble size than the gas flow rate. Therefore, more research should be done on the influence of the liquid flow rate on the bubble size to gain more knowledge on the kinetics of the bubbles and the bubbles behaviour.

The conclusion that is drawn from the experiments on the bubbling efficiency is that for larger particles, higher flow rates are required to get the highest process efficiency. For smaller particles a lower gas flow suffices to acquire a higher efficiency. The bottleneck is to not use a flow rate that is too high, because this will most likely decrease the efficiency due to the increase in turbulence. Another conclusion to be drawn is that the low efficiencies of the process indicate that there is need for improvement on several aspects of the process.

A conclusion that is drawn from executing the experiments is that there is room for improvement of the set-up. This can be done in different aspects as mentioned below. The improvement of this could result in an increase in efficiency of the process.

## 5.2. Recommendations

### 5.2.1 Further research

More research should be conducted on the effect of the liquid flow rate on the efficiency of the extraction process. Because with a higher liquid flow rates more bubbles might be able to pass, and this might increase the interactions between the bubbles and the particles. More of this research could lead to a model for the bubbling efficiency, which can be used to determine the optimal operating conditions for the helium bubbling process. A thing to consider here is that the increase of the liquid flow rate might also increase the turbulence of the flow. This might have negative consequences for the efficiency of the extraction process. This could be examined by using a plexiglass column and making high-speed videos of the bubble behaviour in the column.

Another interesting thing to conduct more research to is the capture of produced foam. The foam that is produced, due to the high viscosity of the mixture and the gas flow, also contains particles that are extracted. In this research the foam was not capture, but it was noticed that this foam does contain particles. This can be done by reducing the foam production or by capturing the foam with a modification of the set-up. As explained in the previous section. Because the foam also extracts particles it would be recommended to use the caption of the foam to improve the efficiency of the process.

### ***5.2.2 set-up***

The set-up could be modified to enhance the efficiency of the process. The gas inlet in the venturi tube is worth modifying, because it fills up with the mixture if the liquid or gas flow stops. This results in particles entering the inlet and precipitating on the bottom of it. This could be acquired by not having the gas inlet all the way around the Venturi tube, but only the top half.

To capture the foam that is formed by the process, the bent tube at the top of the Hallimond tube can be inverted so it faces down. Then a flask could be attached to it to capture the foam in. this way the foam can also be filtered and determine the number of extracted particles in it.

## References

1. World Nuclear Association (2017, December). Generation IV Nuclear Reactors. Retrieved from <http://www.world-nuclear.org/information-library/nuclear-fuel-cycle/nuclear-power-reactors/generation-iv-nuclear-reactors.aspx>
2. Serp, J. et al. (2014). The molten salt reactor (MSR) in generation IV: Overview and perspectives. *Progress in Nuclear Energy*, 77, 308–319. <https://doi.org/10.1016/j.pnucene.2014.02.014>
3. World Nuclear Association (2017, August). Molten Salt Reactors. Retrieved from <http://www.world-nuclear.org/information-library/current-and-future-generation/molten-salt-reactors.aspx>
4. Journee, D. (2014). Helium bubbling in a Molten Salt Fast Reactor, 1–78.
5. Kedl, R. J. (1972). The Migration of a Class of Fission Products (Noble Metals) in the Molten-Salt Reactor Experiment, 96.
6. Fuerstenau, M. C., Jameson, G., & Yoon, R.-H. (2007). *Froth Flotation: A century of innovation*. Littleton: Society for Mining, Metallurgy and Exploration.
7. Robertson, R.C. (1971). Conceptual Design Study of a single-fluid Molten Salt Breeder Reactor, 61-64. Ornl, ORNL-4541
8. Kawatra, S.K. (1995). Froth Flotation – Fundamental Principles Flotation System, 1–30.
9. Centre for minerals research. Flotation. Retrieved from <http://www.cmr.uct.ac.za/cmr/ra/flotation>
10. "flotation process." *The Columbia Encyclopedia*, 6th ed.. . Retrieved June 28, 2018 from Encyclopedia.com: <http://www.encyclopedia.com/reference/encyclopedias-almanacs-transcripts-and-maps/flotation-process>
11. Ulaganathan, V., Javadi, A., Makievski, A. V., Gehin-Delval, C., Pugh, R., Krägel, J., & N. Kovalchuk, R. Miller. (2008). Molecular fundamentals of flotation, 240(2005), 14476.
12. Ghosh, P.. Froth Flotation. Retrieved from <http://www.nptel.ac.in/courses/103103033/module6/lecture6.pdf>
13. Cantor, S. (1973). Density and Viscosity of Several Molten Fluoride Mixtures. *Ornl, ORNL-TM-43*.
14. FlowMaxx Engineering. Venturi Flowmeters. Retrieved from <http://www.flowmaxx.com/venturi.htm>
15. Carter, W.L. (1968). Decay Heat generation by Fission Products and  $^{223}\text{Pa}$  in a Single-Region Molten Salt Reactor. Ornl, ORNL-CF-68-3-38

# Appendix

## A: Results

This appendix contains the tables with the experimental values.

### A.1: Extracted amounts Mo and efficiencies of the experiments.

100 mesh

Time (min)	5 cm <sup>3</sup> /min (g extracted)	15 cm <sup>3</sup> /min (g extracted)	25 cm <sup>3</sup> /min (g extracted)	35 cm <sup>3</sup> /min (g extracted)	45 cm <sup>3</sup> /min (g extracted)
0	0	0	0	0	0
10	0.00087	0.0000667	0.010331	0.005732	0.010264
20	0.002466	0.0000667	0.01413	0.010531	0.015196
40	0.002796	0.0006	0.020462	0.017529	0.023661
80	0.004129	0.0016	0.024794	0.022594	0.026727
Total	0.005462	0.0211	0.0785	0.096292	0.0625
Initial amount added (g)	1.25	1.2736	1.2750	1.2748	1.2736
Efficiency (%)	0.44	1.66	6.15	7.55	4.91

**Table A.1:** Table with yields in grams extracted particles. Also, the efficiency of the process is given. Both are given for each of the gas flows.

170 mesh

Time (min)	5 cm <sup>3</sup> /min (g extracted)	15 cm <sup>3</sup> /min (g extracted)	25 cm <sup>3</sup> /min (g extracted)	35 cm <sup>3</sup> /min (g extracted)	45 cm <sup>3</sup> /min (g extracted)
0	0	0	0	0	0
10	0.001133	0.0014	0.002666	0.015063	0.0016
20	0.006598	0.003799	0.005399	0.020128	0.011464
40	0.008998	0.007465	0.010464	0.02546	0.025394
80	0.016596	0.013197	0.017329	0.031859	0.037124
Total	0.0425	0.0724	0.0785	0.0766	0.0805
Initial amount added (g)	1.2764	1.2731	1.2735	1.2726	1.2765
Efficiency (%)	3.33	5.69	6.16	6.02	6.31

**Table A.2:** Table with yields in grams extracted particles. Also, the efficiency of the process is given. Both are given for each of the gas flows.

3-7 micron

Time (min)	5 cm <sup>3</sup> /min (g extracted)	15 cm <sup>3</sup> /min (g extracted)	25 cm <sup>3</sup> /min (g extracted)	35 cm <sup>3</sup> /min (g extracted)	45 cm <sup>3</sup> /min (g extracted)
0	0	0	0	0	0
10	0.001333	0.003466	0.003399	0.0018	0.008265
20	0.002733	0.009598	0.007265	0.004066	0.013863
40	0.004066	0.013797	0.009931	0.006665	0.019195
80	0.006065	0.015729	0.011597	0.020662	0.027193
Total	0.0296	0.0962	0.0693	0.0443	0.0616
Initial amount added (g)	1.2730	1.2724	1.2734	1.2726	1.2736
Efficiency (%)	2.32	7.56	5.44	3.48	4.84

**Table A.3:** Table with yields in grams extracted particles. Also, the efficiency of the process is given. Both are given for each of the gas flows.

## B: Pictures of other equipment used.

In this appendix the pictures of some of the other equipment can be found to specify which one was used.

### *Pump*



Figure B.1: The Nastec Mida pump, which introduced movement to the liquid.

### *Flowmeter*

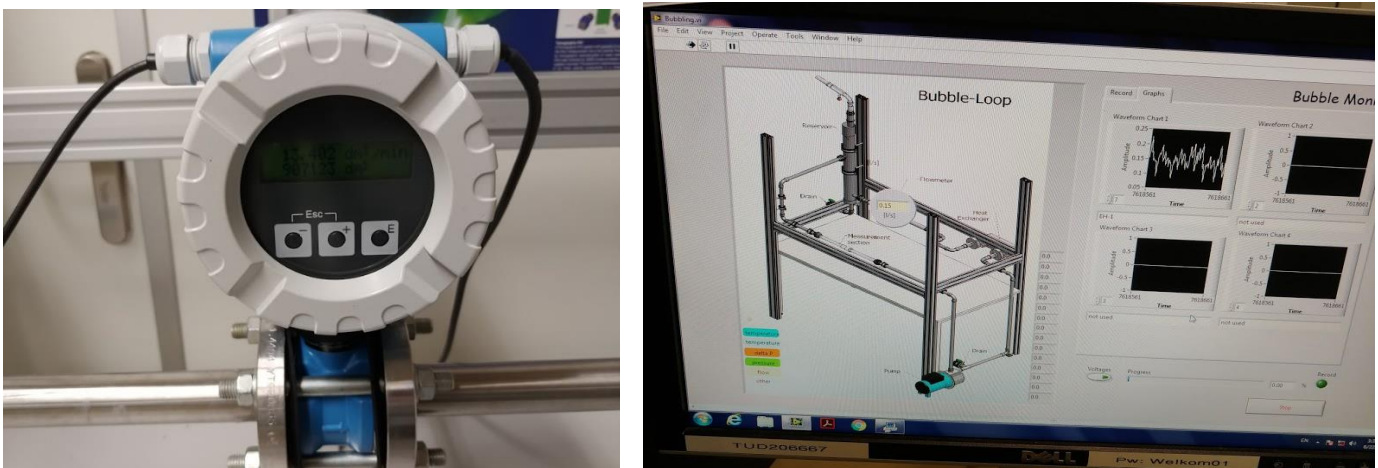


Figure B.2: The flowmeter that kept track of the liquid flow rate. The meter was linked to the computer and used a special made software. The rates on the meter itself are given in  $\text{dm}^3/\text{min}$  and on the computer in  $\text{L}/\text{s}$ .

## *Heat exchanger*



**Figure B.3: Heat exchanger coupled with the loop and 2 tubes which contain the cooling water**

## C: Macros for picture analysis

Fixed Liquid flow rate:

```
1 open("C:/Users/Gijs/Documents/MST/3e jaar/L04/Foto's/Metingen zonder deeltjes/Metingen 12-3-2018/Fixed
2 //setTool("Line");
3 makeLine(2608, 272, 2568, 3440);
4 run("Set Scale...", "known=24.86 unit=unit");
5 //setTool("rectangle");
6 makeRectangle(120, 456, 5376, 2776);
7 run("Crop");
8 run("Subtract Background...", "rolling=50 light");
9 run("Mean...", "radius=2");
10 run("8-bit");
11 run("Enhance Contrast...", "saturated=0.3");
12 setAutoThreshold("Huang");
13 run("Threshold...");
14 setThreshold(0, 205); //205,200,195
15 setOption("BlackBackground", false);
16 run("Convert to Mask");
17 run("Fill Holes");
18 run("Ellipse Split", "binary=40.0cm3(2).JPG add_to_manager add_to_results_table merge_when_relativ_ove
19
20
```

Figure C.1: Macro for the analysis of the fixed liquid flow rate pictures

Fixed Gas flow rate:

```
1 open("C:/Users/Gijs/Documents/MST/3e jaar/L04/Foto's/Metingen zonder deeltjes/Metingen 27-3-2018/30cm3
2 //setTool("Line");
3 makeLine(718, 54, 734, 982);
4 run("Set Scale...", "known=24.86 unit=unit");
5 //setTool("rectangle");
6 makeRectangle(30, 152, 1566, 774);
7 run("Crop");
8 run("Subtract Background...", "rolling=50 light");
9 run("Mean...", "radius=2");
10 run("8-bit");
11 run("Enhance Contrast...", "saturated=0.3");
12 setAutoThreshold("Huang");
13 run("Threshold...");
14 setThreshold(0, 190); //215,210,206,203,195,190
15 setOption("BlackBackground", false);
16 run("Convert to Mask");
17 run("Fill Holes");
18 run("Ellipse Split", "binary=0.56(1).JPG add_to_manager add_to_results_table merge_when_relativ_overla
19 run("Summarize");
20
```

Figure C.2: Macro for the analysis of the fixed gas flow rate pictures